ORIGINAL ARTICLE

Inflammatory Changes in Paravertebral Sympathetic Ganglia in Two Rat Pain Models

Ai-Ling Li[1,2] · Jing-Dong Zhang[1] · Wenrui Xie[1] · Judith A. Strong[1] · Jun-Ming Zhang[1]

Abstract Injury to peripheral nerves can lead to neuropathic pain, along with well-studied effects on sensory neurons, including hyperexcitability, abnormal spontaneous activity, and neuroinflammation in the sensory ganglia. Neuropathic pain can be enhanced by sympathetic activity. Peripheral nerve injury may also damage sympathetic axons or expose them to an inflammatory environment. In this study, we examined the lumbar sympathetic ganglion responses to two rat pain models: ligation of the L5 spinal nerve, and local inflammation of the L5 dorsal root ganglion (DRG), which does not involve axotomy. Both models resulted in neuroinflammatory changes in the sympathetic ganglia, as indicated by macrophage responses, satellite glia activation, and increased numbers of T cells, along with very modest increases in sympathetic neuron excitability (but not spontaneous activity) measured in *ex vivo* recordings. The spinal nerve ligation model generally caused larger responses than DRG inflammation. Plasticity of the sympathetic system should be recognized in studies of sympathetic effects on pain.

Keywords Neuropathic pain · Sympathetic · Macrophage · T cell · Satellite glia · Inflammation · Hyperexcitability

✉ Jun-Ming Zhang
 Jun-Ming.Zhang@uc.edu

[1] Department of Anesthesiology, University of Cincinnati College of Medicine, Cincinnati, OH 45267, USA

[2] Present Address: Department of Psychological and Brain Science, Indiana University Bloomington, 702 N Walnut Grove Ave., Bloomington, IN 47405, USA

Introduction

Peripheral nerve injury can lead to neuropathic pain. Axotomy of peripheral nerves results in well-studied changes in their remote cell bodies, including morphological, metabolic, and electrophysiological changes [1, 2]. Neuropathic pain involves not only neuronal pathways, but also Schwann cells, satellite glial cells in the dorsal root ganglia (DRGs), and cells of the peripheral immune system [3]. In some pain models, it has been proposed that inflammatory processes in an injured peripheral nerve also contribute to pain by affecting adjacent intact axons that were not axotomized by the precipitating injury [4].

Within the peripheral sensory ganglia, an inflammatory reaction can be triggered by injury to remote axons. For example, it is well-known that the satellite glial cells in sensory ganglia become activated, express glial fibrillary acidic protein (GFAP), and proliferate after peripheral nerve injury [5]. DRG satellite glia reactions have also been reported in a model of local inflammation of the DRG, in the absence of overt axon injury [6]. Other examples of inflammatory responses in the DRG include increased macrophage infiltration and activation, as well as T cell infiltration, observed after sciatic or spinal nerve transection [2, 7, 8]. Some of these changes are detectable within days of the axon injury. These neuroinflammatory changes may contribute to the increased excitability of sensory neurons after peripheral nerve injury or local inflammation, for example by increasing cytokines that directly affect neurons [4].

Another component of the peripheral nervous system, the sympathetic nervous system, also plays a role in pain. Some clinical pain conditions are thought to be sympathetically maintained [9, 10], and in several preclinical pain models, blocking sympathetic activity reduces pain (see

[11]). Mechanisms by which the sympathetic nerves might enhance pain include direct excitatory actions on sensory neurons, which develop abnormal adrenergic sensitivity; direct abnormal coupling between the sympathetic and sensory neurons due to sympathetic sprouting within the DRG or at injury sites; and sympathetic regulation of the inflammation process, including direct effects on immune cells [11–17].

Because most peripheral nerves contain a mixture of sensory, motor, and autonomic fibers, many pain models that involve injury of peripheral nerves also lead to injury of sympathetic axons, and/or their exposure to an inflammatory environment within a damaged nerve. Since the sympathetic system can affect pain, it is of interest to know how sympathetic ganglia (SGs) are affected by such pain models. There is an extensive literature on the SG as a model system in which to study peripheral synaptic transmission and the response to peripheral axotomy [18], beginning with classic studies showing "synaptic stripping", i.e. rapid loss of synaptic contact between preganglionic fibers and postganglionic sympathetic neurons after postganglionic axotomy [19]. However, few of these studies have been conducted in the context of pain models. One such study [20] compared the effects of sciatic nerve transection on neuroinflammation in DRGs *versus* lumbar SGs, reporting that GFAP, macrophage, and T cell responses were even stronger in the SG than in the DRG. In addition, there are, to our knowledge, no extensive studies on how the SGs are affected by exposure of their axons to an inflammatory environment in the absence of overt axotomy, as is expected to occur in some pain models and pain conditions.

In this study, we investigated changes in T cells, macrophages, and GFAP expression in lumbar SGs in the spinal nerve ligation (SNL) model (ligation and cutting of the L5 spinal nerve, which also contains sympathetic axons, primarily from SG4 and SG3). To assess the effects on the SG of remote inflammation without axotomy, we compared the effects of SNL on these neuroinflammatory markers to the effects seen after local inflammation of the L5 DRG (LID). This model, which mimics the local inflammation (without axotomy) seen, for example, in certain forms of low back pain, is strongly mitigated by simply cutting the gray rami, the local source of sympathetic fibers in the spinal nerve and nearby DRG [11]. We also determined how these two pain models affected the intrinsic electrophysiological properties of lumbar SG neurons in the ipsilateral SG3 and SG4. Our aim was to begin to investigate the effects of pain models on the SG, because possible alterations in SG properties must be taken into account when evaluating the role of SG neurons in pain.

Materials and Methods

Animals

Sprague–Dawley rats (Harlan, Indianapolis, IN) of either sex or as indicated, weighing 80–200 g, were maintained under a light–dark cycle of 14 h:10 h, with access to food and water *ad libitum*. The experimental protocol was approved by the Institutional Animal Care and Use Committee of the University of Cincinnati. Experiments were conducted in accordance with the guidelines for the treatment of animals of the International Association for the Study of Pain.

Pain Models

Spinal Nerve Ligation (SNL) Model

Animals were anesthetized with 3%–4% isoflurane for induction and 2.5% for maintenance. The depth of anesthesia was confirmed by the absence of withdrawal responses to tail pinch and toe pinch. The lower back was shaved at the incision area and disinfected before surgery. A 3-cm longitudinal incision was made in aseptic skin from L6 to L4 (DRG levels), and the right-side paraspinal muscles were dissected to expose the L4 and L5 spinal nerves. Animals received a unilateral ligation of the right ventral ramus of the L5 spinal nerve according to the description of the SNL model by Kim and Chung [21]. Briefly, the L5 ventral ramus was exposed and tightly ligated using a 6–0 silk suture ~2 to 3 mm distal to the ganglion and cut at the distal end of the suture. In some experiments, a small piece (~0.25 mm^2) of DiI crystal (Life Technologies Carlsbad, CA, catalog D-3911), a lipophilic tracer, was applied at the proximal end of the cut spinal nerve to label the axotomized neurons in the SG. The incision was closed in layers with 4–0 silk. Animals were allowed to recover for 7 days before recording or immunohistochemistry.

Local Inflammation of the DRG (LID) Model

As previously described [22], the L4 and L5 intervertebral foramina were exposed after dissection of the right-side paraspinal muscles. The immune activator zymosan (2 mg/mL, 10 μL, in incomplete Freund's adjuvant) was slowly injected into the L5 intervertebral foramen, above the DRG, through a needle (30-G × ½ inch.), which was bent at a 90° angle 1–2 mm from the tip. During injection, the bent part of the needle was inserted into the intervertebral foramen and kept there for 1–2 min during and after injection to avoid leakage. Animals were allowed to

recover for 3–7 days as indicated before recording or immunohistochemistry.

SG Preparation for Intracellular Recording

Recordings were made in SGs isolated from normal rats, 7 days after SNL, or 3–4 days after LID. Rats were anesthetized with pentobarbital sodium (50 mg/kg, i.p.). A transperitoneal approach was used to identify sympathetic ganglia based on the description by Baron [23]. An incision was made along the abdominal midline approximately from the point of the last rib to the bladder. The internal organs were gently retracted to expose the large vessels (aorta and vena cava) at the midline, underlying which were the sympathetic trunks with ganglia. The ganglia were located very close to the corresponding segmental vessels. After SG3 and SG4 were identified, they were isolated from the surrounding tissue. Oxygenated artificial cerebrospinal fluid (ACSF) (in mmol/L: NaCl 130, KCl 3.5, NaH_2PO_4 1.25, $NaHCO_3$ 24, dextrose 10, $MgCl_2$ 1.2, $CaCl_2$ 1.2, HEPES 16, pH 7.3, bubbled with 95% O_2 + 5% CO_2) was dripped periodically onto the surface of the SGs during the dissection process to prevent hypoxia. The SGs were then placed in a 35-mm Petri dish with oxygenated ACSF and the perineurium removed with fine forceps. The SGs remained in the continuously-oxygenated ACSF for 30 min at room temperature before they were transferred to the recording chamber.

Microelectrode Recording in Whole SG Preparation

Intracellular microelectrode current clamp recordings were made from neurons in whole SG3 or SG4 isolated acutely as described above. The method was similar to that used to record from whole DRG preparations, as detailed in our previous publication [24]. This method allows neurons to be recorded without enzymatic dissociation, leaving the surrounding satellite glia and neighboring neurons intact [25, 26]. The method is similar to that used by others to make microelectrode recordings in isolated whole SGs (e.g. [19, 27]). Whole SGs were placed in a recording chamber which was mounted on the stage of an upright microscope (BX50WI, Olympus, Center Valley, PA). The ganglia were held in place by 2–3 fine nylon threads. The chamber was continuously perfused with oxygenated ACSF at a constant rate of 2–3 mL/min at 36–37 °C. Microelectrode resistance ranged from 40 to 60 MΩ (P-97; Sutter Instruments, Novato, CA). Electrodes were filled with a solution containing (in mol/L) KCl 3, HEPES 0.010, and EGTA 0.010 (pH 7.5). In some recordings from SNL rats, fluorescence was used to identify DiI-labeled axotomized neurons. However, both labeled and non-labeled neurons were recorded and the results were combined.

Immunohistochemistry

At the indicated time points, animals received an intraperitoneal injection of pentobarbital sodium and were transcardially perfused with 0.1 mol/L phosphate buffer followed by 10% formalin in phosphate buffer. SGs were identified and isolated using the anatomical approach described above and then postfixed in 10% formalin in phosphate buffer for another 30 min before being transferred to 30% sucrose. After SGs were embedded in Tissue Freezing Medium (General Data, Cincinnati, OH) and frozen, they were sectioned at 10 μm on a cryostat (CM850, Leica, Buffalo Grove, IL). The SG sections were immunostained for visualization of T cells, macrophages, and GFAP-positive cells including satellite glia and Schwann cells. All staining followed the same procedure but with different antibodies. Briefly, tissue sections were first blocked with 10% normal goat serum followed by overnight incubation with the primary antibody at 4 °C. The next day, they were incubated with the secondary antibody for an hour. In negative control sections, all procedures were the same except the primary antibody was omitted. Images of sections were captured under a fluorescence microscope (BX60WI, Olympus) using Slidebook 6 imaging acquisition software (Intelligent Imaging Innovation, Denver, CO). In quantitative immunohistochemical experiments, sections from all experimental groups were examined in a side-by-side fashion. In isolating SGs for either electrophysiology or immunohistochemistry, we did not encounter fused ganglia in which it was not feasible to separate the ipsilateral from the contralateral side.

T cells

The mouse monoclonal anti-TCR alpha + TCR beta antibody (Abcam, Cambridge, MA, catalog: ab139367) was used as the primary antibody at a dilution of 1:100. The secondary antibody was goat anti-mouse antibody conjugated to Alexa Fluor 594 (Invitrogen, Carlsbad, CA) diluted at 1:500. Stained T cells were quantified by counting the defined objects after threshold adjustment in 4–30 sections for each rat. The density of T cells was computed for each rat as the total number of T cells divided by the total area of sections examined, and is expressed as cells/mm^2. Statistical analysis was performed on the animal values.

GFAP

The primary anti-GFAP antibody was rabbit polyclonal (Immunostar, Hudson, WI, catalog #22522) used at a dilution of 1:100. The secondary antibody was goat anti-

88

Neurosci. Bull. February, 2018, 34(1):85–97

rabbit antibody conjugated to Alexa Fluor 594 (Invitrogen) used at a dilution of 1:1000. To determine the expression of GFAP in SGs, the summed intensities of GFAP were

measured and normalized by the SG area in each analyzed section to give an intensity ratio. The averaged intensity ratios from 7 to 40 images for each animal were used for statistical analysis.

Macrophages

Goat polyclonal anti-Iba1 antibody (Abcam, ab5076) was diluted at 1:500 and used to detect macrophages. The secondary antibody was donkey anti-goat conjugated to Alexa Fluor 594 (Invitrogen) at a dilution of 1:1000. The proportional area was measured as recommended by
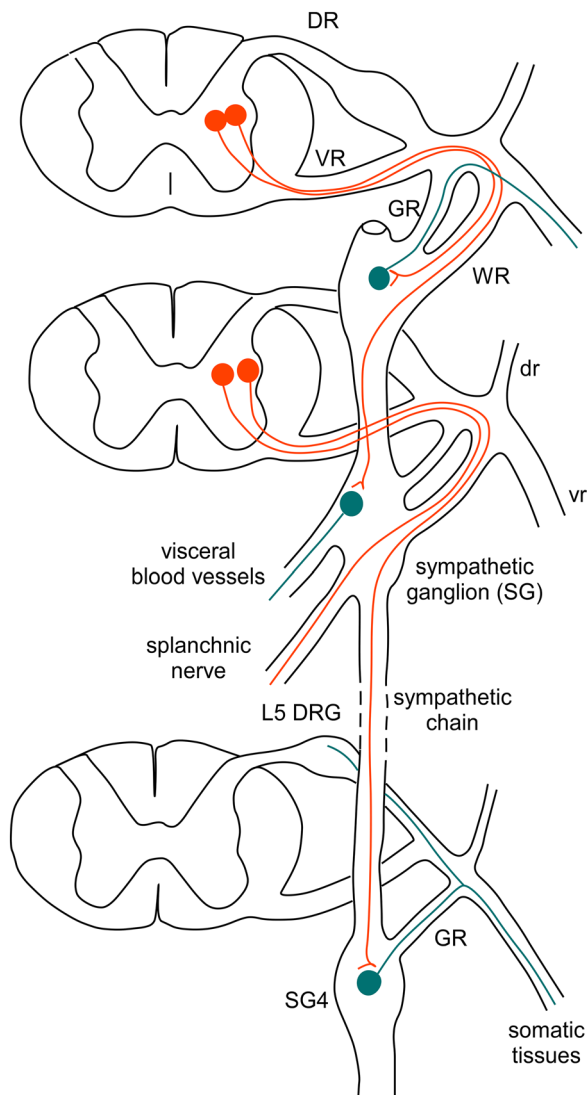

Fig. 1 Schematic diagram of lumbar sympathetic system. Sympathetic preganglionic neurons (*red*) have cell bodies in the intermediolateral cell columns of the spinal cord. Their axons leave the cord through the ventral roots (VR) and follow white rami (WR) to the paravertebral sympathetic ganglion (SG) chain. Some make synapses with postganglionic neurons (*green*) in the paravertebral SGs, either at the same level, or at other levels after projecting in the sympathetic chain. Axons of some preganglionic neurons pass through chain ganglia without synapsing and connect with postganglionic neurons in prevertebral or pelvic ganglia. At the level of the L5 DRG there are no white rami, as preganglionic neurons are found in more rostral regions. Here, postganglionic axons primarily from SG neurons in SG3 (not shown) or SG4 run through the gray ramus (GR) to the L5 spinal nerve, where they may project along the ventral ramus (vr) of the spinal nerve to enter the sciatic nerve and reach peripheral targets, or project into the dorsal ramus (dr) of the spinal nerve, or innervate the region around the L5 DRG itself (primarily innervating blood vessels in normal animals).
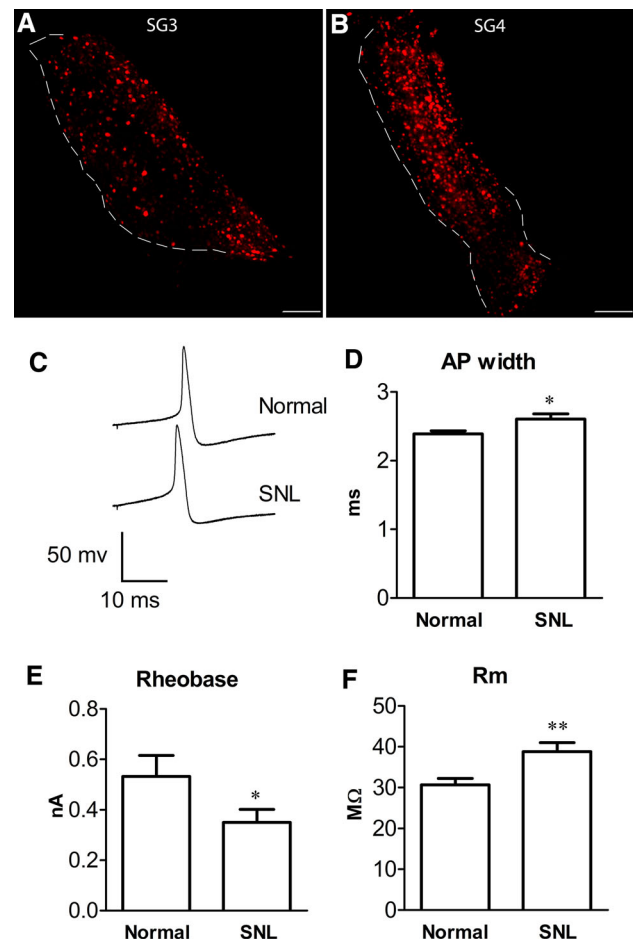

Fig. 2 Effect of L5 spinal nerve ligation (SNL) on excitability of sympathetic ganglionic neurons measured on postoperative day (POD) 7. **A**, **B** Examples of the large numbers of DiI-labeled axotomized neurons in SG3 and SG4, respectively, on POD 7. Dashed lines indicate ganglia borders. *Scale bars*, 250 μm. Images were from whole, unfixed SGs just after microelectrode recording sessions. **C** Representative action potentials (AP) recorded from neurons in isolated whole SG preparations from normal rats and from SNL rats on POD 7. **D–F** Average values of AP duration (**D**), rheobase (**E**), and input resistance (R_m) (**F**). *$P < 0.05$, **$P < 0.01$ compared to the normal group (Mann–Whitney test); $n = 71$ cells in the normal group from 10 male rats and 83 in the SNL group from 14 male rats. Additional electrophysiological values are in Table 1.

Table 1 Electrophysiological parameters of sympathetic neurons in *ex vivo* recordings.

	Normal	SNL	LID
Max dV/dt (V/s)	170.4 ± 6.9	170.2 ± 7.2	185.9 ± 15.1
Threshold (mV)	-32.4 ± 0.9	-32.2 ± 0.8	-34.8 ± 1.9
AP width (ms)	2.39 ± 0.04	$2.61 \pm 0.08*$	2.28 ± 0.09
Peak AP (mV)	24.7 ± 1.2	24.8 ± 1.2	22.4 ± 2.0
Rheobase (nA)	0.53 ± 0.08	$0.35 \pm 0.05*$	0.31 ± 0.09
R_m (MΩ)	30.7 ± 1.5	$38.8 \pm 2.1**$	$43.6 \pm 4.0**$
V_{rest} (mV)	-53.1 ± 1.0	-52.5 ± 1.0	-55.5 ± 1.9
Max # AP	10.3 ± 0.8	10.2 ± 0.8	10.5 ± 1.2
Number of cells	71	83	25

Normal: data from SG3 and SG4 isolated from normal rats. SNL: data from SG3 and SG4 isolated 7 days after L5 spinal nerve ligation. LID: data from SG4 isolated 3–4 days after local inflammation of the DRG.

AP, action potential; Max dV/dt, maximum rate of voltage change during AP upstroke; peak AP, maximum voltage during AP; R_m, membrane input resistance; V_{rest}, resting membrane potential; Max #AP, maximum number of AP evoked by 270 ms suprathreshold stimulus.

* $P < 0.05$; ** $P < 0.01$; significantly different from normal value, Mann–Whitney test.

Donnelly *et al.* [28] as an index of the magnitude of a macrophage response, because the response can include both an increased number of cells and increased ramification of individual cells. Background staining was subtracted and the contrast was slightly enhanced in each section to ensure all labeled cells were measured. The proportional area is expressed as the area of stained macrophage over the SG area in each image. Averaged proportional areas from 6 to 25 images for each rat were used for statistical analysis.

Data Analysis

All statistical analyses were performed using Graphpad Prism software (Graphpad Prism, La Jolla, CA). Two-tailed tests were used throughout. For immunohistochemical data, comparison of values between different groups (normal, sham, and SNL) was done using one-way ANOVA followed by Tukey's *post hoc* test. Because the sham SNL surgery involves a DRG exposure very similar to that used for the LID surgery and had little effect on SG parameters, only sham LID animals were used for comparison to LID animals, and no additional sections from normal animals were obtained. In those experiments, quantification of immunohistochemical data for SGs obtained after LID was compared to SGs from sham LID animals at the same time point, using the *t* test. All statistical analysis of histochemical quantification was based on animal averages. For electrophysiological data, the unpaired *t*-test was used if the data fit a normal distribution or a nonparametric test (Mann–Whitney test) was used if the data failed the D'Agostino and Pearson omnibus normality test. $P < 0.05$ was considered
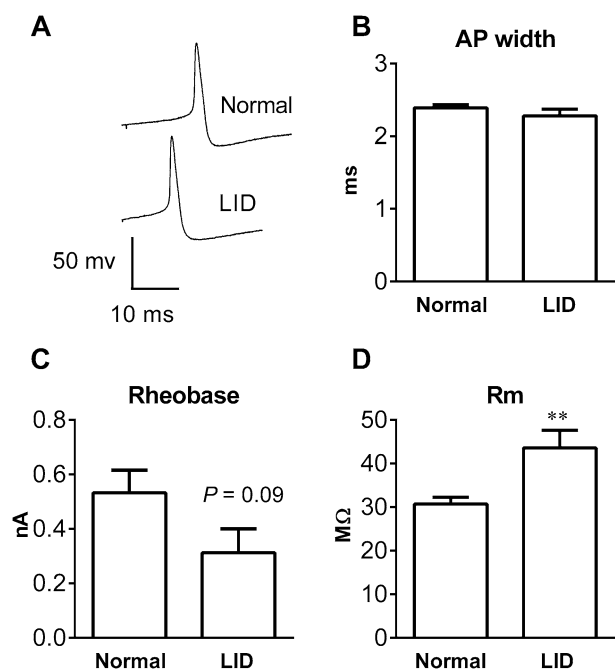

Fig. 3 Effect of local inflammation of L5 DRG (LID) on excitability of sympathetic ganglionic neurons measured on POD 3–4. **A** Representative action potentials (AP) from neurons in isolated whole SG preparations from normal and LID rats on POD 3–4. **B–D** Average values of AP duration (**B**), rheobase (**C**), and input resistance (R_m) (**D**). **$*P < 0.01$ compared with the normal group (Mann–Whitney test), $n = 71$ cells in the normal group (same cells as Fig. 2) and 25 in the LID group (from four male rats). Difference in rheobase approached significance ($P = 0.09$, Mann–Whitney test). Additional electrophysiological values are in Table 1.

significant. Different levels of significance are indicated by the number of symbols: *$P < 0.05$; **$P < 0.01$; ***$P < 0.001$. Data are presented as mean $\pm$ SEM.
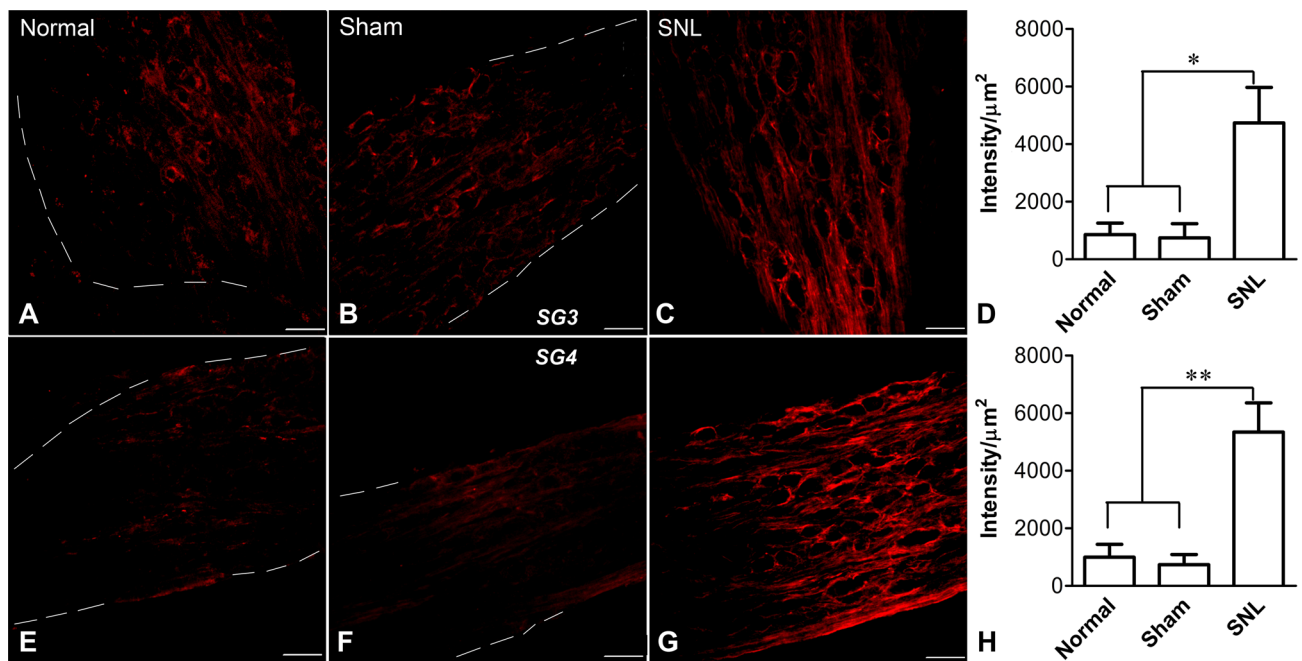
Fig. 4 L5 spinal nerve ligation induced satellite glia activation in both SG3 and SG4. **A–D** Sections of SG3 stained for GFAP in normal (**A**), sham (**B**), and SNL (**C**) rats displayed a large increase in the expression of GFAP in SNL rats. Sections in **B** and **C** were obtained 7 days after SNL or sham SNL surgery. Summary data of fluorescent intensity per square micrometer (intensity/μm^2) revealed no difference between normal and sham rats but a significant difference between sham or normal and SNL rats (**D**; *$P < 0.05$, ANOVA with Tukey's post-test). **E–H** Sections from SG4 in normal (**E**), sham (**F**), and SNL (**G**) animals showed a similarly large increase in GFAP expression in SNL rats. Summary data of intensity/μm^2 showed no difference between normal and sham rats but a significant difference between sham or normal and SNL animals (**H**; **$P < 0.01$, ANOVA with Tukey's post-test). *Scale bars*, 50 μm. Dashed lines indicate ganglia borders. $N = 4$ male rats per group.

Results

The Excitability of Sympathetic Ganglion Cells Increases Modestly After Ligation of the L5 Spinal Nerve

As per the nomenclature of Baron [23], SG4 is the first SG rostral to the L5 DRG. Gray rami connect each sympathetic postganglionic ganglion with the next most caudal DRG (though some of the fibers in the gray rami may course through the sympathetic trunk for one or more levels before entering the gray rami, having their cell bodies in a more distant SG). From the gray rami, a few sympathetic axons turn and enter the DRG region, primarily innervating blood vessels, and a few course through the small dorsal ramus; the majority enter the larger ventral ramus of the spinal nerve to reach their peripheral targets (Fig. 1). As expected from anatomical studies, ligation and cutting of the L5 ventral ramus transected the axons of many cells in the ipsilateral SG4 and SG3: when crystals of the tracer DiI were placed on the transected L5 spinal nerve when the SNL model was implemented, large numbers of neurons in both the ipsilateral SG3 and SG4 were labeled (Fig. 2A, B). Microelectrode recordings in SG3 and SG4 were conducted in ganglia isolated from normal animals or 7 days after ipsilateral L5 SNL. Several measures of excitability increased in the SG after SNL (Fig. 2; Table 1). The action potential was slightly broadened, and the rheobase was reduced, which probably reflected an increase in resting input resistance, as threshold and resting potential were not changed. Other electrophysiological parameters were not significantly affected (Table 1).

The Excitability of Sympathetic Ganglion Cells is Less Affected by Local Inflammation of the L5 DRG

We also examined the electrophysiological properties of SG4 neurons after local inflammation of the adjacent L5 DRG. To correspond with previous studies of hyperexcitability in DRG neurons after local inflammation, we chose days 3–4 as the time point for these experiments. As shown in Fig. 3 and Table 1, the changes in excitability were more modest than those in the SNL model. Only the increase in input resistance reached significance. Trends towards hyperexcitability did not reach significance, e.g. the decrease in rheobase ($P = 0.09$) and reduction in threshold ($P = 0.058$).
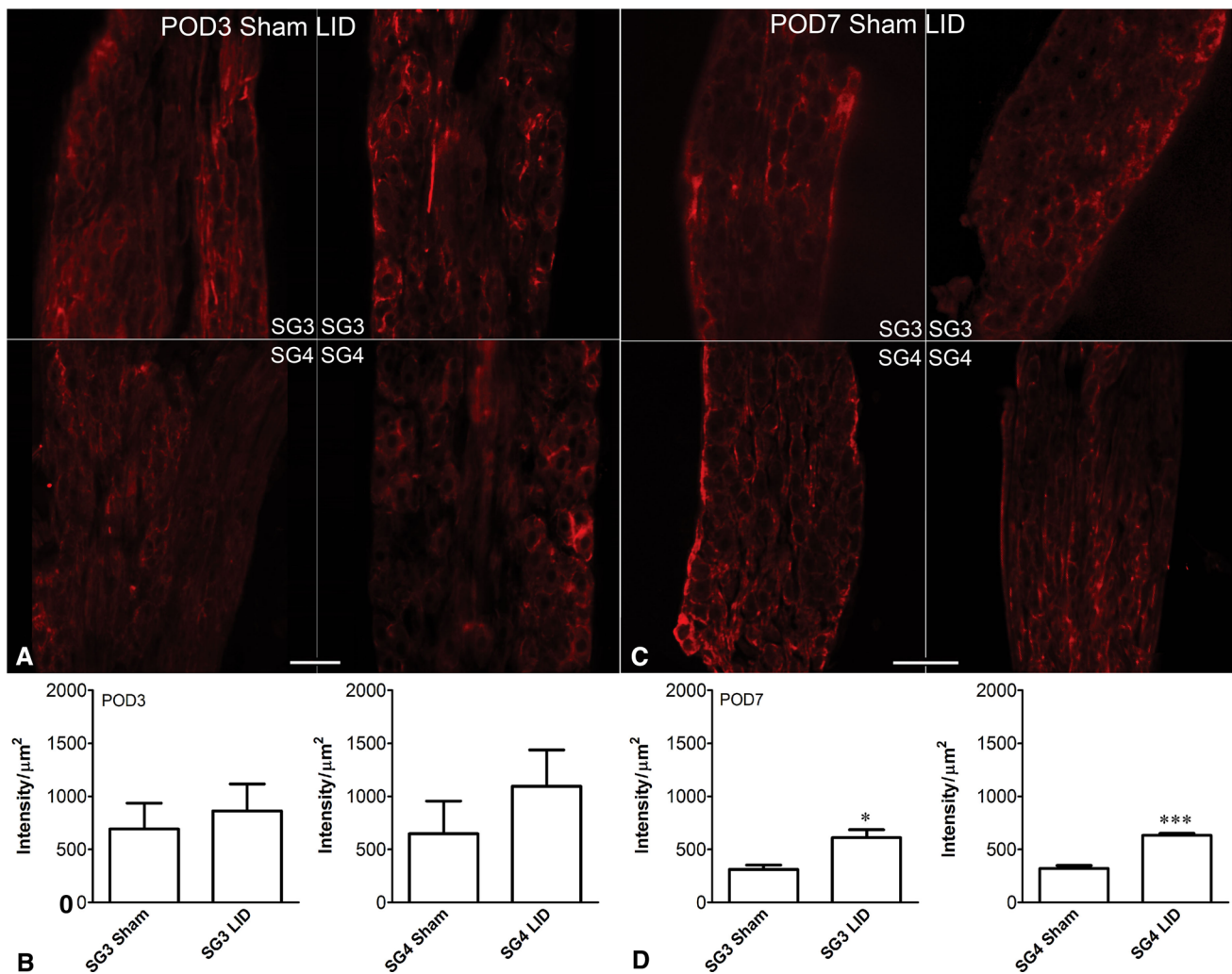
Fig. 5 Local inflammation of the L5 DRG induced more modest satellite glia activation in SG4. **A–D** Sections of SG3 and SG4 obtained 3 days (**A**) or 7 days (**C**) after LID or sham LID surgery and immunostained for GFAP (*Scale bars*, 50 μm). Summary data showed no significant GFAP upregulation in either SG3 or SG4 by day 3 (**B**). For sections obtained on day 7, summary data showed significant upregulation (**D**; *$P < 0.05$, ***$P < 0.001$ between sham and LID groups, *t*-test). However, the degree of upregulation was much smaller than that induced by SNL at the same time point (compared to Fig. 4) ($n = 4$–5 rats of both sexes per group).

Compared to Local DRG Inflammation, Spinal Nerve Ligation Induced Greater Activation of Satellite Glial Cells in Both L3 and L4 SGs

Immunohistochemical analysis of GFAP levels was used as a measure of satellite glial activation [29]. The expression of GFAP was significantly increased in both SG3 and SG4 7 days after the SNL surgery. Quantitatively, the degree of upregulation appeared similar between SG3 and SG4 (Fig. 4), with an upregulation >5-fold. There was no significant difference between normal and sham SNL groups.

In contrast, the upregulation of GFAP after DRG inflammation was much less and only reached significance on day 7, when ~2-fold upregulation was found (Fig. 5).

Spinal Nerve Ligation and DRG Inflammation Modestly Increased the Macrophage Response in Sympathetic Ganglia

Macrophage responses in the SG were assessed using the general macrophage marker Iba-1. The response was measured as the proportion of section area that expressed Iba-1, and was significant in both SG3 and SG4 at 7 days after SNL (Fig. 6). The increase was ~2-fold in SG4 and slightly less in SG3. Sham SNL surgery did not have any significant effect. In the LID model (Fig. 7), similar fold-increases were found on both days 3 and 7, but the responses were more variable and reached significance only on day 7 in SG4, when the response increased ~2.5-fold.
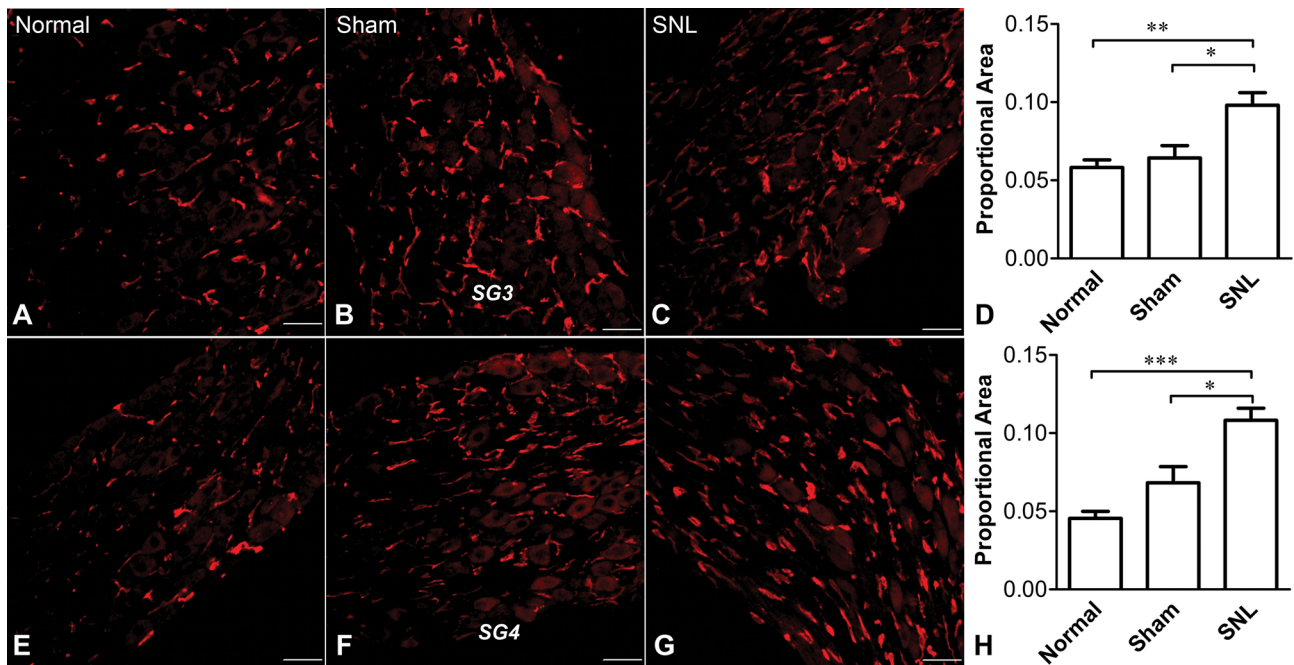
Fig. 6 L5 spinal nerve ligation evoked infiltration/activation of macrophages in both SG3 and SG4. **A–D** Sections of SG3 stained with Iba-1 in normal (**A**), sham (**B**), and SNL (**C**) rats showed activation of macrophages in SNL rats on POD 7. The summary data (**D**) of the proportion of total area labeled by Iba-1 (Proportional Area) revealed no significant difference between normal and sham, but significant differences between those groups and the SNL group. **E–H** Similar findings were obtained in sections from SG4 in normal (**E**), sham (**F**), and SNL (**G**) rats. Summary data indicated no significant difference between normal and sham, but both groups were significantly lower than the SNL group (**H**). $*P < 0.05$, $**P < 0.01$, $***P < 0.001$ between indicated groups (ANOVA with Tukey's post-test); $n = 4$ male rats per group; *scale bars*, 50 μm.

Spinal Nerve Ligation More so than DRG Inflammation Significantly Increased the Number of T Cells in SGs

There were generally very few T cells in the normal and sham SNL groups, except that one sham rat showed a density of T cells comparable to the lower values in SNL rats in SG3. Due to this higher variability, the ∼24-fold increase in T cells 7 days after SNL in SG3 did not quite reach significance (ANOVA, overall $P = 0.0595$). In SG4, the T cell density increased 33-fold over normal (Fig. 8). T cell increases were also found in the SGs after LID, but these were more modest, never significantly increasing >5-fold over sham LID values (Fig. 9; note difference in scale from Fig. 8). The pattern of T cell staining also differed between the two models; in the SNL model T cells were scattered throughout the ganglia including near neuronal cell bodies, while in the LID model the T cells tended to be more numerous near the edges of the ganglion.

Discussion

We observed signs of neuroinflammation and modest neuronal hyperexcitability in the lumbar sympathetic ganglia in two pain models: ligation of the L5 spinal nerve (SNL); and local inflammation of the L5 DRG (LID), in which an inflammatory stimulus was placed near the L5 DRG but there was no axotomy. In general, the inflammatory and electrophysiological changes were milder in the LID model than in the SNL model. The macrophage responses in the SG were similar in both models, but the T cell response, satellite glial response, and increased neuronal excitability were larger after SNL. Only SNL involved axotomy, which affected a large fraction of the neurons in SG4 and SG3. Since previous studies of electrophysiological and inflammatory changes in the SG have focused on the key role of axotomy, and especially loss of target-derived neurotrophins, it is perhaps not surprising that SNL led to larger changes than LID. However, it is instructive that LID also caused some inflammatory changes in the nearby SG. It is not yet known whether these effects are due to proximity of the inflammatory stimulus to the SG cell bodies, or whether local inflammation around the SG axons in the region of the inflamed L5 DRG provides a signal that is transmitted to the SG. The overall similarity of findings in the SG4 *versus* the more distant SG3 suggests the latter mechanism may play at least some role. The findings may be of relevance to other pain models involving partial peripheral nerve injury, in which spared SG axons would presumably be exposed to local inflammation at the injury site.
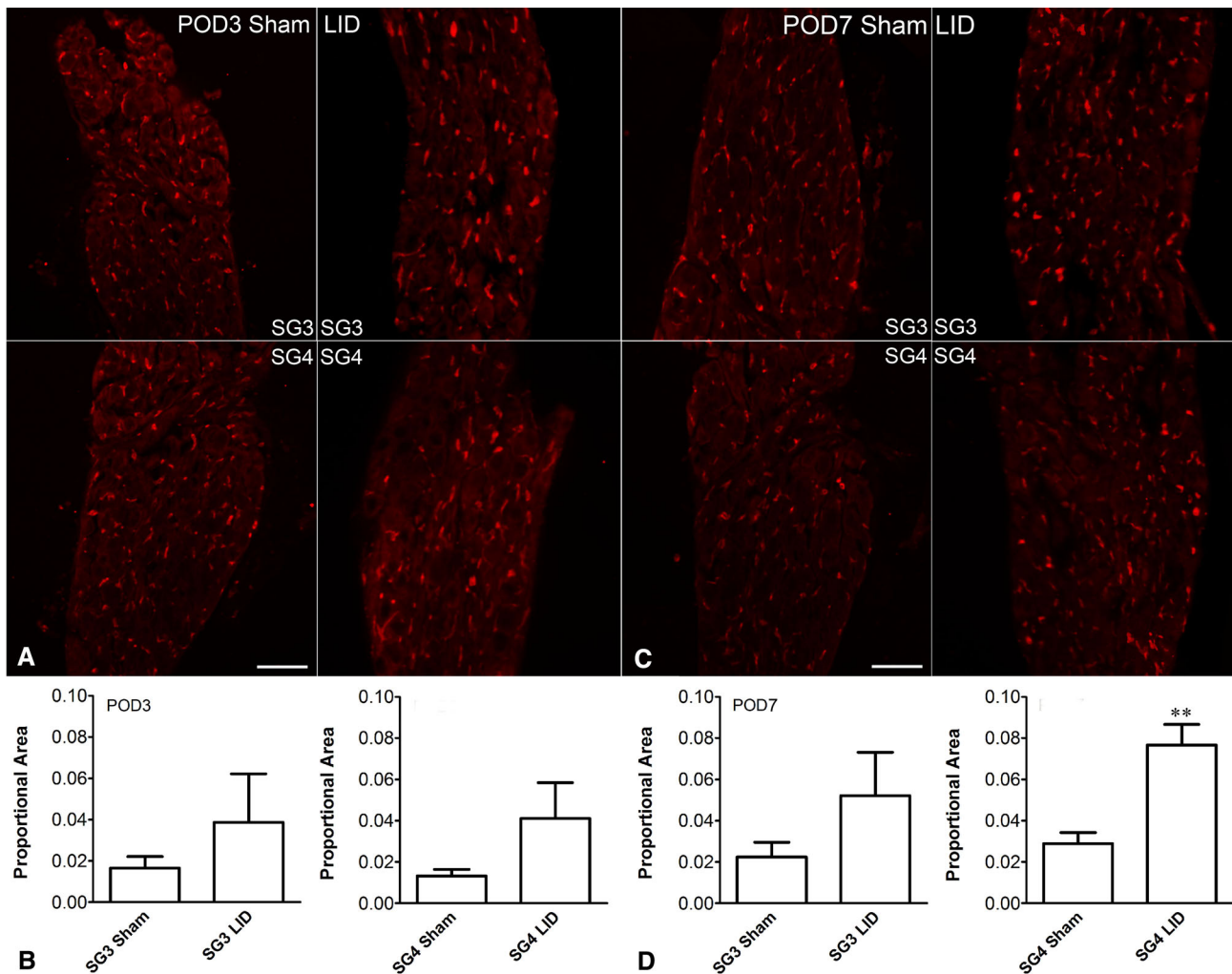
Fig. 7 Effect of local inflammation of DRG 5 (LID) on macrophage infiltration/activation in SG3 and SG4. Sections of SG3 and SG4 from rats 3 (**A**) and 7 days (**C**) after LID or sham LID immunostained with the macrophage marker Iba-1. **B** Summary data indicated that the increase in Iba-1 did not reach significance in either SG on day 3. **D** Summary data indicated a significantly higher Iba-1 signal on day 7, only in SG4. **$P < 0.01$ between the two groups, *t*-test; $n = 4–5$ rats of either sex per group; *scale bars*, 50 μm.

The activation of satellite glial cells, as indicated by increased GFAP immunoreactivity, has been reported to occur around both axotomized and non-axotomized SG cells within one day following sciatic nerve transection [20]. Our study demonstrated that activation occurred for at least 7 days after either SNL (a more proximal injury than that used in [20]) or local DRG inflammation. The larger response to SNL suggests that axotomy is a stronger but not necessary signal for the activation of satellite glial cells. The function of SG satellite glia is less well understood than that of DRG satellite glia. However, possible functional consequences of this activation are suggested by studies showing that the sympathetic satellite glia may be phagocytic, may influence synaptic transmission and purinergic signaling, and may play a role in mediating the loss of synaptic transmission from preganglionic inputs that occurs after axotomy [29]. A role for

macrophages in synaptic stripping in the SG has also been proposed. It will be of interest to determine whether DRG inflammation (or other conditions affecting the SG without axotomy) also modifies synaptic transmission to SG neurons from preganglionic inputs. Macrophages have also been proposed to help mediate the regeneration responses of axotomized SG cells [18]. By extrapolating from studies of DRG neurons, it might be expected that macrophages in the SG could release molecules that increase the excitability of SG neurons [30]. Macrophage invasion of the SG can also be induced by systemic toxins that affect the SG terminals and cause them to lose contact with their targets. It has been proposed that this is because, like axotomy, such toxins disrupt the transport of peripheral trophic factors to the soma [31].

The very low number of T cells in naïve SGs is similar to that in DRGs [8]. T cell increases in the SG have also
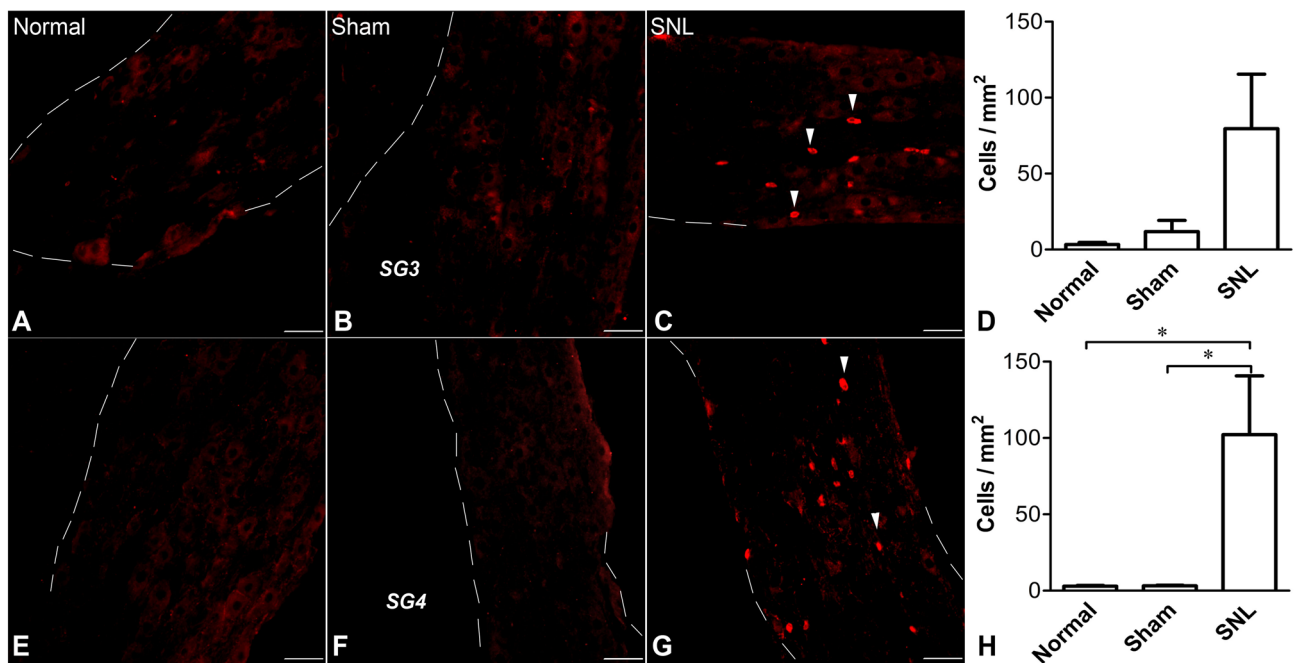
Fig. 8 Effect of L5 spinal nerve ligation on infiltration of T cells in SG3 and SG4 on POD 7. **A–D** SG3 sections stained with an antibody to the T cell receptor (TCR) in normal (**A**), sham (**B**), and SNL (**C**) rats. The statistical analysis of TCR-positive cells/μm² revealed that the differences between normal, sham, and SNL rats (**D**) did not quite reach significance (ANOVA, P = 0.0595). **E–H** SG4 sections stained for TCR in normal (**E**), sham (**F**), and SNL (**G**) rats showing that significantly more T cells were recruited in SNL SG4 than sham or normal rats (**H**; *P < 0.05, ANOVA with Tukey's post-test). Dashed lines indicate ganglia borders. Arrowheads indicate individual T cells. (n = 4 male rats per group; scale bars, 50 μm).

been reported after sciatic nerve transection, an effect lasting at least 10 weeks. This was reported to be larger than the influx into DRGs [20]. As is the case for macrophages, a hyperexcitability-promoting effect of invading T cells might be expected, by analogy with the better understood effects on DRG neurons (depending on the subtype of T cell that predominates) [30].

The changes in excitability we recorded in SG neurons were relatively small, compared to for example the large increases in L5 DRG neurons after SNL [32] or local inflammation [33]. However, in both of those studies, myelinated (Aβ) DRG neurons showed much larger increases in excitability than unmyelinated (C) DRG neurons. The SG neurons, which are also unmyelinated, are perhaps similar to C cells from the DRG in their responses to these pain models. When one considers only the unmyelinated DRG neurons, LID induces only a small increase in action potential duration [33], while SNL leads to a larger increase in action potential duration and a decreased rheobase [32]. In particular, the marked spontaneous activity in DRG neurons after either SNL or LID is largely confined to myelinated Aβ cells. In the present study, we also failed to find significant spontaneous activity in isolated SG neurons after either SNL or LID. Spontaneous activity was rarely recorded, and generally consisted of only 1 or a few action potentials over a 1-min period.

This contrasts with the very high frequency bursting activity in spontaneously-active myelinated DRG neurons in these pain models as reported under similar recording conditions [32, 33]. Our study may have been better suited to record any spontaneous activity in SGs than some previous electrophysiological studies because our study was conducted at temperatures close to body temperature rather than at room temperature; in DRG neurons spontaneous activity is very temperature-sensitive [34].

Relatively small changes in intrinsic SG neuronal excitability have also been reported in previous studies of the effects of axotomy on sympathetic neurons in the superior cervical ganglia, in contrast to the dramatic loss of presynaptic input (synaptic stripping) found in those studies [19, 27]. The latter occurs very rapidly, starting within one day. The decline in synaptic input is very large (e.g. a 70% decline in evoked synaptic potentials) so, although the decreased rheobase/increased input resistance we recorded after SNL would tend to counteract the effects of declining excitatory synaptic input, it would clearly be unable to completely compensate for such a loss. The present study in conjunction with the previous studies raises the question of how axotomized sympathetic neurons have such marked effects on pain behaviors, if they have a dramatic decrease in presynaptic drive and are not spontaneously active. It is generally assumed that
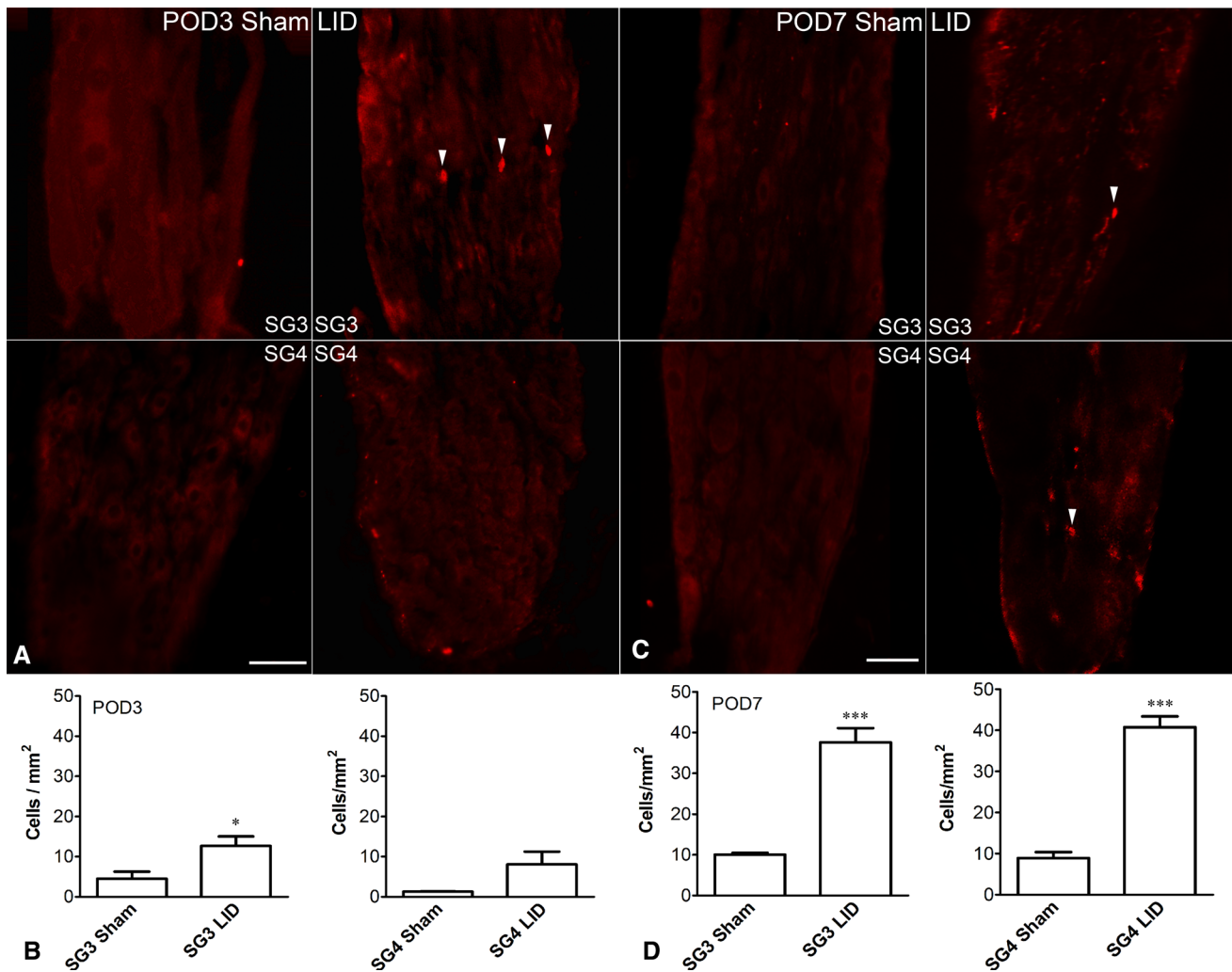
Fig. 9 Effect of local inflammation of L5 DRG (LID) on T cell infiltration in SG3 and SG4. Sections of SG3 and SG4 at POD 3 and POD 7 immunostained with T cell receptor antibody. **A** Representative microimages from POD 3 animals showing a small increase in T cells after LID. **B** Statistics for cells/mm^2 from both SG3 and SG4 sections showed only the SG3 increase reached significance. **C** Representative immunostaining of T cell receptor 7 days after LID.

D Statistics for cells/mm^2 from both SG3 and SG4 showing a significant difference between groups, but the absolute values were much smaller than those after SNL (compared with Fig. 8). Arrowheads indicate examples of individual T cells. (*$P < 0.05$, ***$P < 0.001$ between groups, t-test; $n = 4$ rats of either sex per group; *scale bars*, 50 μm).

sympathetic neurons require presynaptic drive in order to fire and release transmitter onto their peripheral targets. Thus, after L5 SNL, or sciatic nerve transection, one would assume that the axotomized neurons in SG4 and SG3 were no longer able to release neurotransmitters. Yet, removing SG3 and SG4 reduces the degree of inflammation induced in lumbar DRGs by subsequent sciatic nerve transection [35], suggesting functionality of some of these SG neurons despite the large loss of synaptic drive that would be expected to occur after sciatic nerve transection, based on the previous axotomy studies. In addition, in the SNL model, pain behaviors are markedly decreased by additionally cutting the gray rami to the L4 and L5 DRGs (a procedure which would predominantly disconnect the

already axotomized SG neurons from the region of those DRGs, by giving them a second axotomy a few millimeters proximal to the axotomy incurred during SNL) [24]. In that study, it was proposed that this antinociceptive effect is explained by loss of sympathetic sprouting into the axotomized DRG, which was shown to occur largely from SG axons in the small dorsal ramus that are not axotomized in SNL but are axotomized when the gray rami are cut. This explanation, relying on the role of non-axotomized SG neurons, might also account for some of the findings in the study by McLachlan and Hu [35]. It is interesting that, in their study of sympathetic effects on DRG inflammation induced by sciatic nerve transection, decentralization of SG3 and SG4 (i.e., cutting the preganglionic inputs by

transecting the sympathetic chain proximal to L3) was somewhat less effective in reducing DRG inflammation than complete removal of SG3 and SG4 [35]. This is consistent with a pro-inflammatory role of SG neurons that escape axotomy after sciatic nerve transection, even if they are a relatively small fraction of the total SG3/SG4 neurons. Another possible mechanism to consider is that there is intrinsic spontaneous activity of SG neurons *in vivo* that is not captured by *ex vivo* recording (for example, perhaps because of washout of local inflammatory mediators), or that the assumption of required presynaptic drive of the SG needs to be reconsidered. Finally, we must consider the possibility that the previously-described synaptic stripping after axotomy of the sympathetic neurons in the superior cervical ganglia is larger than that in the lumbar paravertebral ganglia.

The original study on synaptic stripping [19] found that only axotomized SG neurons showed massive synaptic loss, while adjacent non-axotomized neurons retained normal synaptic inputs (as in experiments when only one of several nerve branches was injured). This suggests that extensive synaptic stripping of the SG is unlikely in the LID model, in which case the neuroinflammation and increased membrane resistance we found in SGs would be better positioned to enhance the output of the postganglionic neurons than in the SNL model.

The antinociceptive behavioral effects of cutting the gray rami to the L4 and L5 DRGs are even more dramatic in the context of the LID model [11]. A primary mechanism of this effect is the large reduction in the inflammation process that occurs with removal of these sympathetic fibers, as evidenced by reduction in DRG macrophage infiltration and the pro-inflammatory cytokine profile. The present study suggests that in this model, as well as other pain models, the sympathetic neurons cannot be considered as passive, unchanging players. Instead, they may also undergo functional changes as a result of either axotomy or exposure of their axons to a peripheral inflammatory environment, and the possible ramifications of this plasticity require further investigation in specific pain models and conditions.

References

1. Kreutzberg GW. Reaction of the neuronal cell body to axonal damage. In: Waxman SG (ed.). The Axon: Structure, Function and Pathophysiology. New York: Oxford University Press, 1995: 355–374.
2. Navarro X. Chapter 27: Neural plasticity after nerve injury and regeneration. Int Rev Neurobiol 2009, 87: 483–505.
3. Scholz J, Woolf CJ. The neuropathic pain triad: neurons, immune cells and glia. Nat Neurosci 2007, 10: 1361–1368.
4. Moalem G, Tracey DJ. Immune and inflammatory mechanisms in neuropathic pain. Brain Res Brain Res Rev 2006, 51: 240–264.
5. Hanani M. Satellite glial cells in sensory ganglia: from form to function. Brain Res Brain Res Rev 2005, 48: 457–476.
6. Xie WR, Deng H, Li H, Bowen TL, Strong JA, Zhang JM. Robust increase of cutaneous sensitivity, cytokine production and sympathetic sprouting in rats with localized inflammatory irritation of the spinal ganglia. Neuroscience 2006, 142: 809–822.
7. Hu P, McLachlan EM. Distinct functional types of macrophage in dorsal root ganglia and spinal nerves proximal to sciatic and spinal nerve transections in the rat. Exp Neurol 2003, 184: 590–605.
8. Hu P, McLachlan EM. Macrophage and lymphocyte invasion of dorsal root ganglia after peripheral nerve lesions in the rat. Neuroscience 2002, 112: 23–38.
9. Drummond PD. Sensory-autonomic interactions in health and disease. Handb Clin Neurol 2013, 117: 309–319.
10. Borchers AT, Gershwin ME. Complex regional pain syndrome: a comprehensive and critical review. Autoimmun Rev 2014, 13: 242–265.
11. Xie W, Chen S, Strong JA, Li AL, Lewkowich IP, Zhang JM. Localized sympathectomy reduces mechanical hypersensitivity by restoring normal immune homeostasis in rat models of inflammatory pain. J Neurosci 2016, 36: 8712–8725.
12. Baron R. Peripheral neuropathic pain: from mechanisms to symptoms. Clin J Pain 2000, 16: S12–S20.
13. Padro CJ, Sanders VM. Neuroendocrine regulation of inflammation. Semin Immunol 2014, 26: 357–368.
14. Pertin M, Allchorne AJ, Beggah AT, Woolf CJ, Decosterd I. Delayed sympathetic dependence in the spared nerve injury (SNI) model of neuropathic pain. Mol Pain 2007, 3: 21.
15. Pertovaara A. The noradrenergic pain regulation system: a potential target for pain therapy. Eur J Pharmacol 2013, 716: 2–7.
16. Xie Y, Zhang JM, Petersen M, LaMotte RH. Functional changes in dorsal root ganglion cells after chronic nerve constriction in the rat. J Neurophysiol 1995, 73: 1811–1820.
17. Zhang JM, Song XJ, LaMotte RH. An *in vitro* study of ectopic discharge generation and adrenergic sensitivity in the intact, nerve-injured rat dorsal root ganglion. Pain 1997, 72: 51–57.
18. DeFrancesco-Lisowitz A, Lindborg JA, Niemi JP, Zigmond RE. The neuroimmunology of degeneration and regeneration in the peripheral nervous system. Neuroscience 2015, 302: 174–203.
19. Purves D. Functional and structural changes in mammalian sympathetic neurones following interruption of their axons. J Physiol 1975, 252: 429–463.
20. Hu P, McLachlan EM. Inflammation in sympathetic ganglia proximal to sciatic nerve transection in rats. Neurosci Lett 2004, 365: 39–42.
21. Kim SH, Chung JM. An experimental model for peripheral neuropathy produced by segmental spinal nerve ligation in the rat. Pain 1992, 50: 355–363.
22. Xie W, Strong JA, Kim D, Shahrestani S, Zhang JM. Bursting activity in myelinated sensory neurons plays a key role in pain behavior induced by localized inflammation of the rat sensory ganglion. Neuroscience 2012, 206: 212–223.
23. Baron R, Janig W, Kollmann W. Sympathetic and afferent somata projecting in hindlimb nerves and the anatomical organization of the lumbar sympathetic nervous system of the rat. J Comp Neurol 1988, 275: 460–468.
24. Xie W, Strong JA, Zhang JM. Increased excitability and spontaneous activity of rat sensory neurons following in vitro stimulation of sympathetic fiber sprouts in the isolated dorsal root ganglion. Pain 2010, 151: 447–459.

25. Zhang JM, Song XJ, LaMotte RH. Enhanced excitability of sensory neurons in rats with cutaneous hyperalgesia produced by chronic compression of the dorsal root ganglion. J Neurophysiol 1999, 82: 3359–3366.

26. Song XJ, Hu SJ, Greenquist KW, Zhang JM, LaMotte RH. Mechanical and thermal hyperalgesia and ectopic neuronal discharge after chronic compression of dorsal root ganglia. J Neurophysiol 1999, 82: 3347–3358.

27. Sacchi O, Rossi ML, Canella R, Fesce R. Synaptic and somatic effects of axotomy in the intact, innervated rat sympathetic neuron. J Neurophysiol 2006, 95: 2832–2844.

28. Donnelly DJ, Gensel JC, Ankeny DP, van Rooijen N, Popovich PG. An efficient and reproducible method for quantifying macrophages in different experimental models of central nervous system pathology. J Neurosci Methods 2009, 181: 36–44.

29. Hanani M. Satellite glial cells in sympathetic and parasympathetic ganglia: in search of function. Brain Res Rev 2010, 64: 304–327.

30. Moalem G, Tracey DJ. Immune and inflammatory mechanisms in neuropathic pain. Brain Res Rev 2006, 51: 240–264.

31. Schreiber RC, Shadiack AM, Bennett TA, Sedwick CE, Zigmond RE. Changes in the macrophage population of the rat superior cervical ganglion after postganglionic nerve injury. J Neurobiol 1995, 27: 141–153.

32. Xie W, Strong JA, Zhang JM. Local knockdown of the NaV1.6 sodium channel reduces pain behaviors, sensory neuron excitability, and sympathetic sprouting in rat models of neuropathic pain. Neuroscience 2015, 291: 317–330.

33. Xie W, Tan ZY, Barbosa C, Strong JA, Cummins TR, Zhang JM. Upregulation of the sodium channel NaVβ4 subunit and its contributions to mechanical hypersensitivity and neuronal hyperexcitability in a rat model of radicular pain induced by local DRG inflammation. Pain 2016, 157: 879–891.

34. Li H, Liu B, Dobretsov M, Brull SJ, Zhang JM. Thermosensitivity of large primary sensory neurons. Brain Res 2002, 926: 18–26.

35. McLachlan EM, Hu P. Inflammation in dorsal root ganglia after peripheral nerve injury: effects of the sympathetic innervation. Auton Neurosci 2014, 182: 108–117.